Journal of proteome research

Article

Metabolomics Analysis of Effects of Commercial Soy-based Protein Products in Red Drum (*Sciaenops ocellatus*)

Fabio Casu, Aaron M. Watson, Justin Yost, John W. Leffler, Thomas Gibson Gaylord, Frederic T. Barrows, Paul A. Sandifer, Michael R. Denson, and Daniel W. Bearden

J. Proteome Res., **Just Accepted Manuscript** • DOI: 10.1021/acs.jproteome.7b00074 • Publication Date (Web): 14 Jun 2017

ACS Publications

Journal of Proteome Research is published by the American Chemical Society. 1155 Sixteenth Street N.W., Washington, DC 20036

Metabolomics Analysis of Effects of Commercial Soy-based Protein Products in Red Drum (*Sciaenops ocellatus*)

Fabio Casu[†], *Aaron M. Watson*[‡], *Justin Yost*[‡], *John W. Leffler*[‡], *Thomas Gibson Gaylord*[§], *Frederic T. Barrows*[#], *Paul A. Sandifer*[¶1], *Michael R. Denson*[‡], *and Daniel W. Bearden*[†*]

† Hollings Marine Laboratory, National Institute of Standards and Technology, Chemical Sciences Division, 331 Fort Johnson Road, Charleston, South Carolina 29412, U.S.A.

‡Marine Resources Research Institute, South Carolina Department of Natural Resources, 217 Fort Johnson Road, Charleston, South Carolina 29412, U.S.A.

§Bozeman Fish Technology Center, United States Fish and Wildlife Service, 4050 Bridger Canyon Road, Bozeman, Montana 59715, U.S.A.

#United States Department of Agriculture, Agricultural Research Service, Hagerman Fish Culture Experiment Station, 3059F National Fish Hatchery Road, Hagerman, Idaho 83332, U.S.A.

¶Hollings Marine Laboratory, National Oceanic and Atmospheric Administration, 331 Fort Johnson Road, Charleston, South Carolina 29412, U.S.A.

*Corresponding author.

[1]Present address: Hollings Marine Laboratory, College of Charleston, 331 Fort Johnson Road, Charleston, South Carolina 29412, U.S.A.

ABSTRACT: In this study, we investigated the metabolic effects of four different commercial soy-based protein products on red drum fish (*Sciaenops ocellatus*) using Nuclear Magnetic Resonance (NMR) spectroscopy-based metabolomics along with unsupervised principal component analysis (PCA) to evaluate metabolic profiles in liver, muscle and plasma tissues. Specifically, during a 12-week feeding trial, juvenile red drum maintained in an indoor recirculating aquaculture system were fed four different commercially available soy formulations, containing the same amount of crude protein, and two reference diets as performance controls: a 60 % soybean meal diet that had been used in a previous trial in our lab and a natural diet. Red drum liver, muscle, and plasma tissues were sampled at multiple time points to provide a more accurate snapshot of specific metabolic states during the grow-out. PCA score plots derived from NMR spectroscopy data sets showed significant differences between fish fed the natural diet and the soy-based diets, both in liver and muscle tissues. While red drum tolerated the inclusion of soy with good feed conversion ratios, a comparison to fish fed the natural diet revealed that the soy-fed fish in this study displayed a distinct metabolic signature characterized by increased protein and lipid catabolism, suggesting an energetic imbalance. Furthermore, among the soy-based formulations, one diet showed a more pronounced catabolic signature.

KEYWORDS: aquaculture, metabolomics, NMR, red drum, *Sciaenops ocellatus,* soy

INTRODUCTION

Fish constitutes an important source of protein in the human diet worldwide. Aquaculture is one of the fastest growing food-producing sectors, currently accounting for approximately 50 % of the world fish destined for human consumption, and the share is expected to rise to nearly 60 % by 2030. [1] One of the major challenges of aquaculture is its sustainability largely due to the fact that several cultured species are carnivorous, thus requiring the utilization of large quantities of fishmeal, which in turn is produced from wild fish. [2] Attempts to overcome this limitation have led to the evaluation of alternative feeds for aquaculture species with partial or total replacement of fishmeal as the major protein source with animal by-products and proteins derived from plants such as cereal grains, legumes and oilseeds. [3, 4] Soybean-based feeds have been the focus of several studies. [5-9]

Soybean (*Glycine max* Linnaeus) is the most widely utilized plant-based protein source in aquafeeds, and it is largely processed to produce oil, thereby yielding a cake of high protein content. Typically, this product is further processed to derive a series of soybean derivatives, such as soy protein concentrates (SPC), soy protein isolate (SPI), soy flour and soybean meal (SBM). [10] Soy protein products are considered good candidates as replacements for fishmeal due to their high crude protein content and reasonably balanced amino acid composition. Nevertheless, the use of soy proteins as feedstuff ingredients for fish aquaculture faces some important challenges, mainly the different levels of essential amino acids (EAA) and presence of anti-nutritional factors (ANF), such as trypsin inhibitors, saponins, non-starch polysaccharides (e.g., raffinose and stachyose) and phytic acid, which can adversely affect feed utilization and fish

growth [10, 11] in a species-specific manner. It has been shown that the sulfur-containing amino acids (methionine and cysteine) and lysine are present at lower concentrations in SBM than in fishmeal, although adequate supplementation with synthetic amino acids is common based on previously determined minimum requirement estimates. [10, 12, 13]

One example of fish species that has been shown to tolerate relatively high levels of soy products in their diets is red drum (*Sciaenops ocellatus*). [14] Red drum has shown aquaculture potential and the development of alternative feeds with reduced fishmeal content could assist in lowering the high production costs of commercial aquaculture by reducing feed costs as long as the dietary efficiency is maintained. When testing new ingredients for aquaculture feed development, reliable high-throughput quantitative techniques with a high degree of reproducibility are necessary for the evaluation of the effects of the different dietary regimes on fish metabolism and subsequent effects on growth. One such highly reproducible, quantitative, and unbiased technique is Nuclear Magnetic Resonance (NMR) spectroscopy-based metabolomics.

Metabolomics is the study of the global profile of endogenous metabolites (low molecular weight molecules) that are present within an organism or biological sample (the *metabolome*). The metabolome is affected by multiple factors including environmental conditions as well as diet. [7, 15, 16] Metabolomics has been successfully applied to studies focused on assessing the response of aquatic species to different stressors (e.g. toxicity, disease, temperature and diet). [17, 18] NMR spectroscopy is a powerful analytical technique that is widely used for the identification and quantification of macromolecules and small organic molecules and is particularly useful for the study of complex mixtures from biological samples. NMR spectroscopy-based metabolomics can

be applied to the field of aquaculture for the evaluation of the effect of experimental diets on the fish metabolic profiles. [19] In the study presented here, we used an NMR spectroscopy-based metabolomics approach to evaluate the effects of different commercially available soy formulations on juvenile red drum (*Sciaenops ocellatus*) maintained in an indoor recirculating aquaculture system over the course of a 12-week feeding trial. Multiple metabolic pathways related to energy production were significantly affected by the different dietary treatments. Collectively, our results suggest that feed formulations containing high levels of alternative ingredients to fishmeal, specifically soy-containing diets, still require optimization for productive outcomes in aquaculture.

EXPERIMENTAL SECTION

Animal Husbandry and Dietary Treatments

Captive, wild red drum broodstock were volitionally spawned at the Marine Resources Research Institute (MRRI) in Charleston, South Carolina, by the South Carolina Department of Natural Resources (SCDNR). Larval fish grown from a single unique genetic family were grown to juvenile size and transported to the Hollings Marine Laboratory (HML) in Charleston, South Carolina to an indoor, semi-recirculating seawater system where they were distributed into twenty-four 1,100 L 1.52 m diameter experimental tanks at a density of 35 fish/tank (See *Supporting Information, Part I* for additional details). Subsequently, fish were fed twice daily to satiation on a pelleted soy-free conditioning diet (Table S1 – *Supporting Information*) for one month prior to the start of the experiment. The fish mean weight at the beginning of the feeding experiment

was 90.6 g ± 3.8 g. All tanks were batch weighed on Day 0, and 3 fish per tank were randomly selected and individually processed for the T_0 time point (See *Sample Collection* below). For subsequent weeks (weeks 2 to 5 and 9 to 12), treatments were split into 2 groups (A and B), which were alternated weekly to minimize handling stress.

Six diets (four experimental diets and two reference diets) were randomly assigned to four tanks per treatment, and during the study each diet was sampled (n = 12 fish total from two separate tanks) weekly to provide weekly monitoring of the metabolome. The experimental diets were fishmeal-free and consisted of different formulations of commercially available soy products (diets #2-5) containing high quantities of soy ingredients (>40 g/100 g of feed) (Table S1, *Supporting Information*). All experimental diets were isonitrogenous, isolipidic and isoenergetic with 40 % nominal total crude protein and 15 % nominal total crude lipid. Tanks were siphoned and any excess feed was removed from the tanks after 10 min of no visible feeding. Fish were not fed on sampling days.

Additional fish were sacrificed at the end of the 12-week study for whole-body (n = 5 fish/treatment) and fillet composition (n = 5 fish/treatment). Proximate analysis on the whole body and fillets was performed by the Clemson University Feed and Forage Laboratory (Clemson, South Carolina) (Tables S2 and S3, *Supporting Information*).

Sample Collection

Fish tissues were collected within approximately 5 min post-mortem following anaesthetization by immersion in tricaine methane-sulfonate (MS-222, Argent Labs) (lethal dose of 500 mg/L for at least 3 min). Fish were dissected anteriorly from anus to

gills and viscera were removed intact. Liver was excised and rinsed with cold isotonic water (3 % saline) to remove blood, placed in pre-labeled cryovials, flash frozen in liquid nitrogen and transferred to a -80 °C freezer for storage until homogenization.

Subsequently, the right fillet was dissected, the skin removed, and the fillet washed with cold isotonic water (3 % saline). Using an 8 mm biopsy punch, five plugs of fillet were extracted from above the lateral line, near the dorsal fin and head, placed in pre-labeled cryovials, flash frozen in liquid nitrogen, and transferred to a -80 °C freezer for storage, until further processing.

Details for plasma collection are given in the *Supporting Information, Part I.*

Quality control materials included extraction blanks, a liver control material (LCM), a muscle control material (MCM), and control plasma (CP) from pooled excess tissues previously collected from red drum, and stored at -80 °C until use. Additionally, NIST Standard Reference Materials, SRM 1946 ("Lake Superior Fish Tissue") and SRM 1950 ("Metabolites in Human Plasma") were used as reference control materials. SRM samples were stored at -80 °C until use. Vials containing the quality control materials were thawed on ice prior to use and extracted in each batch alongside the experimental samples.

Metabolite Extraction for NMR Spectroscopy Analysis

Frozen liver and muscle samples were individually homogenized using a cryogenic ball-mill (Retsch, Inc., Newtown, PA, USA) and 10 mL, 25 mL, and 35 mL grinding jars with 15 mm or 20 mm stainless steel balls, while keeping the samples constantly frozen by operating in a liquid nitrogen cryogenic cart (Chart Industries, Inc., Garfield Heights,

OH, USA). After homogenization, tissues were aliquoted by weighing 100 mg (± 3 mg)/sample, transferred to 2 mL ceramic bead tubes (2.8 mm) (Mo Bio Laboratories, Carlsbad, CA, USA) and stored at -80 °C until extraction.

The wet tissue extraction method used was a modified version of the chloroform:methanol:water extraction technique introduced by Bligh and Dyer [20-22] with slight modifications to account for different water content in each type of tissue, a method that has been extensively used in our laboratory. [7, 23] Proper personal protective equipment was used and safety precautions for handling chloroform as indicated on the Safety Data Sheets (SDS) were followed to protect laboratory staff from exposure to chloroform, a known grade II carcinogen. Chloroform (4 mL/g wet weight for both liver and muscle) and Millipore DI water (2 mL/g wet weight for both liver and muscle) were pre-mixed in 10 mL glass centrifuge tubes (Corning Inc., Corning, NY, USA) with screw caps (Kimble Chase, Vineland, NJ, USA) and pre-chilled on ice. Ice-cold methanol (4 mL/g wet weight for both liver and muscle) was added to frozen wet tissue samples in ceramic bead tubes followed by ice-cold Millipore DI water (0.83 mL/g wet weight for muscle; 1.09 mL/g wet weight for liver) and homogenized using a bead beater (2 cycles at 6500 rpm for 20 s/cycle) (Precellys 24, Bertin Corp., Rockville, MD, USA). The polar homogenates were then transferred to the glass centrifuge tubes containing the premixed chilled water/chloroform mixture. The final solvent volume ratio was chloroform:methanol:water (2:2:1.8, v/v/v). The resulting mixture was vortexed for 30 s and incubated on ice for 10 min. Samples were then centrifuged at 2000 *g* for 5 min at 4 °C. Three layers were visible. The polar phase (top layer) was then carefully transferred into new pre-weighed Eppendorf tubes and dried using an Eppendorf Vacufuge

(Eppendorf, Hauppauge, NY, USA) for approximately 2.5 h to 3 h until dry. A total of 600 μL of NMR buffer (100 mmol/L phosphate buffer in D_2O, pH 7.3, with 1.0 mmol/L sodium 3-(trimethylsilyl)propionate 2,2',3,3'-d (TMSP) as internal chemical shift reference) was added to each dried sample, the samples were then vortexed for a few seconds until completely dissolved and centrifuged. Approximately 550 μL of the resulting solution were then transferred into 5 mm NMR tubes (Bruker Biospin, Inc., Billerica, MA, USA) for subsequent NMR spectroscopy analysis.

Details for plasma processing are given in the *Supporting Information, Part I.*

NMR Spectroscopy Data Acquisition

Approximately 2376 samples (liver, muscle, plasma, and quality controls) were prepared and analyzed by proton NMR spectroscopy for this study. Furthermore, NMR spectra such as ^{13}C- heteronuclear single quantum coherence (HSQC) experiments were collected on selected samples to aid compound identification. All NMR experiments were performed at 298 K on a Bruker Avance II 700 MHz spectrometer (Bruker Biospin) equipped with a 5 mm triple-resonance, z-gradient TCI cryoprobe and a refrigerated holding-stage SampleJet autosampler. Additional details regarding the NMR spectroscopy may be found in the *Supporting Information, Part I*.

NMR Spectral Analysis and Multivariate Statistical Data Analysis

Metabolites were identified based on 1D ^{1}H, 2D ^{1}H-^{1}H JRES, and 2D ^{1}H-^{13}C NMR experiments and the Birmingham Metabolite Library was used for comparison of 2D ^{1}H-^{1}H JRES spectra. [24] Identities were based on comparison of chemical shifts and spin-spin

couplings with reference spectra and tables noted in published reports, [25] the Human Metabolome Database (HMDB, http://www.hmdb.ca), [26] the Biological Magnetic Resonance data Bank (BMRB, http://bmrb.wisc.edu/), [27] an in-house compiled database, and Chenomx® NMR Suite profiling software (version 8.1; Chenomx, Inc., Edmonton, Canada). Most often metabolite identification was achieved at a Level 2, putative identification level. [28] Spectral features that could not be identified based on database or literature searches are annotated as "Unknown".

For multivariate statistical analysis, the spectra were divided into a series of bins (buckets) with a bin width of 0.005 ppm in the range of δ 10.0 ppm to 0.2 ppm and certain spectral regions were excluded because of artifacts due to water suppression or because of contaminants that appeared in our blank sample spectra. NMR spectra were then scaled to the sum of total spectral intensities to minimize sample variability due to the amount of tissue extracted. Generally, principal component analysis (PCA) was conducted on appropriate subsets of the data with appropriate class labeling of the subsets to aid in visual pattern recognition. Pareto normalization, with mean centering of the bins was used in all cases to account for the sometimes wide dynamic range of spectral feature intensity. PCA score plots were assessed for meaningful groupings and groups were assessed for significant differences using ± 1 Standard Error of the Mean (SEM) error bars and Student's t-tests (two-tailed, unequal variance). Binning, scaling, and PCA analysis were performed using AMIX 3.15 (Bruker Biospin). For the PCA loading analysis, the 95th percentile of absolute intensity was used as an arbitrary threshold to select approximately 100 NMR spectral features (signals), which represent the metabolites that significantly change in one direction or the other.

Quality control samples were analyzed in each batch along with experimental samples. QC samples included extraction blanks, composite materials from the study, standard reference materials (SRMs), and replicate extraction samples. To assess the analytical variation of our methods, QC sample spectra were evaluated for spectral relative standard deviation (RSD = standard deviation/mean x 100 %). [29]

Statistical Analyses

The effects of experimental treatments on growth performance parameters were compared using a linear regression model within R statistical software (v3.0.3, R core Team, 2013) with significance level set to $P = 0.05$).

The effects of experimental treatments on metabolite levels were compared using Student's t-test (normally distributed data) or Wilcoxon test (non-normally distributed data), and one-way ANOVA with significance levels determined using Tukey's post-hoc test, with critical limits set to $P < 0.05$.

RESULTS AND DISCUSSION

Aquaculture Production Characteristics

Standard production characteristics (described below) from the feeding study show that there were not dramatic differences in growth outcomes among the four experimental diets or the 60 % soybean meal reference diet (diet #1), but the natural reference diet did significantly outperform all of the pelleted diets as expected, with the soy-based feeds performing at less than 50 % of the natural diet based on fish average weights per time point (Figure S1, *Supporting Information*).

Growth Performance and Feed Utilization

We detected a significant difference in feed consumption among treatments (ANOVA, $P = 0.021$) with diet #4 showing significantly higher feed consumption per fish than diet #2 (Table S4, *Supporting Information*). Despite this difference, weight gain (g gained/fish), final weight, final length, feed conversion ratio (FCR) (see footnotes of Table S4, *Supporting Information* for definitions), specific growth ratio (SGR), and condition factor (K) were all found not to be significantly different across treatments. The natural diet was not included in these statistical analyses; however, all natural diet parameters were found to significantly outperform all experimental feeds when a separate ANOVA was run (data not shown).

Although all of the experimental soy-based feeds performed at less than 50 % of the performance of their theoretical maximum (based on the natural diet) under these experimental conditions, several encouraging results were observed. Feed conversion ratios for three of the four experimental feeds were below 2, indicating favorable digestibility and absorption of nutrients from the feeds. The ability of the fish to retain consumed protein from the feeds as measured by the protein efficiency ratio (PER) for the experimental feeds (an indicator that the fish were readily able to digest and utilize the available protein in the diets) was possibly higher in 4 of the 5 experimental diets than that calculated for the natural diet. These results suggest that, when using high soy-based feeds, one potential area for improvement may be palatability or some other factor related to the presentation of the pelleted diets.

Proximate Biochemical Composition

Proximate and mineral compositions of whole body tissue as well as fillet tissues from each treatment were determined (Tables S2 and S3, *Supporting Information*). Dry matter content was significantly lower in the whole body tissue from diet #1 than diets #3 and #5 ($P = 0.007$). No significant differences were observed in whole body protein, fat, or ash between treatments. Fillet protein was significantly higher in diet #3 compared to all other dietary treatments, with no other significant differences between treatments. Fillet ash content was significantly lower in diet #2 when compared to diets #1 and #4, but was not significantly different from diets #3 or #5. Both phosphorous and calcium in the whole body tissue exhibited similar patterns of significance between treatments with diet #2 being significantly lower than diet #5 with all other dietary treatments showing intermediate values between diets #2 and #5, and not significantly different from each other or diets #2 and #5. Potassium was found to be significantly higher in diet #4 than diets #2 and #5. Diet #2 was also significantly lower in potassium concentration than diet #3. No significant differences in other minerals were observed. No significant differences were detected in fillet dry matter, fat or any of the minerals.

Eviscerated Body Weight and HSI

Eviscerated body weights (g) and hepatosomatic index (HSI) for each treatment at the conclusion of the 12-week feeding study (n=12 per dietary treatment) were determined (Table S5, *Supporting Information*). There was no significant difference among treatments for eviscerated body weight (ANOVA, $P = 0.183$). HSI was significantly

different between treatments (ANOVA, $P = 0.002$). Diet #2 resulted in a significantly higher HSI than diets #1, #3, and #4 but was not significantly different from diet #5.

Metabolomics Quality Control Assessment

The pooled control materials (LCM, MCM, and CP), standard reference materials (SRM 1946 and SRM 1950) and replicate extraction samples for liver, muscle, and plasma were evaluated for spectral relative standard deviation (RSD) (Figures S2, S3, and S4, *Supporting Information*). Quantiles of the % RSD derived from the QC sample NMR spectra (See *Supporting Information, Part I* for additional details and the QC summary in Table S6, *Supporting Information*) indicate a high degree of control for the analytical variability of the measurements.

Metabolomics Trajectories Analysis

Red drum liver and muscle tissues as well as plasma were analyzed using multivariate statistical analysis; specifically, principal component analysis (PCA) was used to examine the time evolution of the metabolome.

The liver, muscle, and plasma tissue samples from nine time points (T_0, T_2, T_3, T_4, T_5, T_9, T_{10}, T_{11}, T_{12}; n = 12 for each diet at each time point) were analyzed for each of the four experimental diets, the natural diet, used as a reference for theoretical maximum performance, and diet #1 as the pelleted control (Figure 1; Figures S5 and S6, *Supporting Information*). The total explained variance in PC1 and PC2 was approximately 60 % to 70 % for all models.

Liver: The PCA score plots for the natural diet show a clear trajectory which progresses from left to right with time (Figure 1). This trajectory moves steadily to the right for the first few weeks of the study (T_2 to T_4), but starting from about week 5 until week 12, it stabilizes around a single locus, despite a 60 % growth based on average fish weight during this period of time (Figure S1, *Supporting Information*). These results indicate that red drum fed on the natural diet reach some sort of metabolic equilibrium around week 5 to week 12 of feeding. The soy formulations (diets #1 through #5) similarly move steadily to the right of the score plot, although less rapidly compared with the natural diet, requiring 3 weeks to 4 weeks to develop an intermediate metabolic profile, which significantly differs from the initial state as represented by T_0. These diets seem to reach homeostasis around week 9 to week 12, despite a 14 % growth based on average fish weight during the same period of time (Figure S1, *Supporting Information*).

Muscle: As far as the natural diet is concerned, the explained variance in PC1 alone is 65.6 % and appears to be dominated by the difference in metabolic profiles between the metabolic state at T_0 and the time points T_2 to T_{12} (Figure S5, *Supporting Information*). This observed difference does not seem to be specific to the natural diet, and, although to a lesser extent, it was detected for all diets analyzed and it likely originated from the metabolic response to a stressor (e.g., changes in temperature, adaptation to a different diet, etc.), which occurred early in the experiment. In general, for the experimental diets there was no significant difference along PC1 among time points T_9 to T_{12}, once again suggesting that a stable metabolic state is reached around week 9.

Plasma: The larger variability detected for each diet/time point makes the appreciation of any significant trends in the plasma data difficult and further analysis is necessary (Figure S6, *Supporting Information*).

Collectively, the results from PC1/PC2 score plots indicate that liver and muscle tissues from fish fed the five soy-based experimental diets and the natural diet display strong time-dependent metabolic trajectories; however, the plasma data does not display discernable metabolic trajectories even though our data quality assessment seems to be more than adequate.

Interestingly, as suggested by the liver metabolic trajectories, while fish fed the natural diet undergo rapid metabolic changes, which are already detectable at week 2 of the 12-week study, a longer period of time of 3 weeks to 4 weeks is required to detect any significant differences for red drum fed soy-based diets. Additionally, for all soy-based diets in this study, a metabolic equilibrium which remains stable throughout the remainder of the study is reached around week 9, thus suggesting that short-term feed studies on red drum in this size class and culture environmental conditions when fed soy-based diets should not be shorter than 9 weeks to 12 weeks of growth. Similar principles may apply to other species; however the specific time frames will likely be largely dependent on the specific fish species, growth conditions, and feed formulations adopted in the study.

Metabolomics End-point Analysis

We subsequently focused on the comparison amongst the six diets based on the end-points of the metabolic trajectories by combining time points T_9 through T_{12}, in an effort

to investigate whether the observed trend in the liver and muscle metabolomic profiles showed consistent patterns among the experimental diets. Combining time points T_9 to T_{12} was justified based on the observed homeostasis for all tissues at weeks 9 to 12; additionally, this combination allowed for an increase in the numerical strength of the resulting PCA models.

A PCA score plot comparing T_0 and T_{end} for all diets for the liver tissue (Figure S7, *Supporting Information*) had a total explained variance along PC1 and PC2 of 64.4 % (50.5 % along PC1 only). In all cases, a significant separation between T_0 and T_{end} samples was detected along the first principal component. A PC1 loading analysis (Figures S8A and S8B, *Supporting Information*) showed 11 compounds with significant differences between T_0 and T_{end} samples. Specifically, T_0 samples showed significantly higher levels of ascorbate, glucose, glycerol 3-phosphate and melibiose; however, the same samples displayed significantly lower levels of alanine, glutamate, glutamine, glutathione, glycogen, maltose, and taurine when compared with the samples at T_{end}. (Table S7, *Supporting Information*).

Particularly interesting was the detection of significant levels of melibiose, a disaccharide generated from partial hydrolysis of raffinose, in the T_0 liver samples. Raffinose is an oligosaccharide composed of galactose, glucose, and fructose, known to be present at high concentrations in different vegetables, beans, and whole grains. The chemical linkage between galactose and glucose is at the α-1,6 position and its hydrolysis requires highly specific enzymes (α-galactosidases) not present in fish (or other monogastric animals), but produced only by bacteria that are part of their gut microbiome. The presence of melibiose in fish at T_0 suggests that the conditioning diet

might have induced significant changes in the composition of the gut microbiome, thus allowing for the production of this disaccharide and its accumulation in the liver. Despite the presence of raffinose at significant amounts in soy beans (~ 1.5 %), none of our soy-based experimental diets showed significant amounts of melibiose in liver tissues at T_{end}, possibly suggesting that within the 5 weeks to 9 weeks required for red drum to reach metabolic homeostasis, composition of the gut microbiome has changed with subsequent loss of α-galactosidase-producing bacteria.

Subsequently, time point T_0 was excluded from the analysis in order to focus on the end-point (T_{end}) differences among the experimental treatments. Accordingly, PCA score plots for liver and muscle tissues were generated.

Liver and muscle T_{end} analysis: The first two principal components (PC1 and PC2) together explained 46.5 % of the total variance for the liver (Figure 2A) and 63.8 % for the muscle (Figure 2B). The liver and muscle samples showed a significant difference ($P < 0.001$) in metabolic profiles between the natural diet and the experimental diets (diet #2 through #5) along PC1, whereas no significant differences were detected between diets #2 to #5 and diet #1 (pelleted control). Additionally, these models clearly indicate that among the different experimental diets, diet #2 is significantly different from the other four soy formulations.

A new PCA model was therefore generated, which excluded the natural diet, to further investigate the differences among the soy-based experimental diets in the liver and muscle tissues (Figures 2C and 2D). These new models have total combined explained variances in PC1 and PC2 of 41.9 % and 63.7 % for liver and muscle, respectively. These

plots display a distinguishable separation ($P < 0.05$) between diet #2 and the other four soy-based diets along the first principal component for both tissues.

Loading Analysis and Metabolite Identification for T_{end} Data

Liver: The PC1 loading plot derived from the liver PCA (Figure 2A) was analyzed in an attempt to identify the specific metabolites that drive the separation along PC1 between fish fed the natural diet and those fed the experimental soy-based diets (Figure 3A and 3B). Seventeen compounds were identified (level 2) [28] which along with 7 unidentified features were significantly different between the two dietary regimes. Our NMR data (Table 1) revealed that when compared to fish fed the natural diet, red drum fed the experimental soy formulations were generally characterized by significantly lower levels of the following metabolites: the amino acids sarcosine and threonine, metabolites involved in energy production such as glucose, organic acids/osmolytes such as lactate and N, N-dimethylglycine, the tricarboxylic acid (TCA) cycle intermediate succinate and the dicarboxylic acid malonate, in addition to the phospholipid O-phosphocholine. On the other hand, increased levels of the following metabolites were detected in the experimental soy-based diets when compared to the natural diet: the amino acids glycine and alanine, β-alanine, energy compounds glycogen, maltose and glycerol 3-phosphate, and the organic acid/osmolyte taurine. In particular, the glycine content was 2.5-fold higher in the soy-based diets compared with the natural diet; additionally, glycerophosphocholine and glycerol 3-phosphate were 1.6- and 1.4-fold higher, respectively (Figure 4A and Table 1). In contrast, dimethylglycine, sarcosine, and

malonate were significantly lower (0.08, 0.10, and 0.13-fold change over the natural diet).

Muscle: Similar to the liver tissue, a PC1 loading plot was calculated from the muscle score plot (Figure 2B) to determine which metabolites are responsible for the separation along PC1 between the natural diet and the experimental soy-based diets (Figure 5A and 5B). Fifteen metabolites were identified (level 2) [28] in the filtered loading plot (Table 1). Our data indicate that the metabolites betaine, lysine, ornithine, and trimethylamine N-oxide (TMAO) were generally lower in red drum fed the experimental soy-based diets while alanine, glycine, serine, histidine, 4-hydroxyproline, ATP, creatine, creatine phosphate, carnitine, and malate were higher compared with the natural diet. Fold changes of metabolite levels compared with the natural diet are shown (Figure 4B and Table 1). Strikingly, glycine levels were approximately 8- to 9-fold higher in muscle tissue of fish fed the soy-based diets compared with those fed the natural diet. In contrast, TMAO, ornithine and lysine were significantly lower (0.22, 0.23, and 0.24-fold change over the natural diet).

Diet #2: From the PCA models for red drum liver and muscle tissues (Figure 2A and 2B), it is apparent that diet #2 separates from the other soy-based experimental diets and therefore, the PC1 loading plot derived from the model which excludes the natural diet (Figure 2C) was analyzed to identify the metabolites that are responsible for the observed separation along PC1 in the liver (Figure 3C and 3D). Our results show that red drum fish fed diet #2 were characterized by higher levels of metabolites such as glucose, glycogen, maltose, glycerol 3-phosphate, and serine, whereas they displayed lower concentrations of alanine, glutamate, glutamine, glutathione, O-phosphocholine and

taurine (Table 2) compared to experimental control diet #1, and diets #3, #4 and #5. In particular, fish fed diet #2 showed the highest levels of glycerol 3-phosphate, and the lowest levels of O-phosphocholine in the liver tissue among all soy-based diets analyzed (Figure 6 and Table 2).

Analysis of the PC1 loading plot (Figure 5C and 5D) derived from the muscle model in Figure 2D revealed that red drum fed diet #2 generally displayed higher levels of metabolites such as asparagine, glycine, histidine, proline, 4-hydroxyproline, serine, threonine, anserine, carnitine, ATP and lactate, whereas they showed lower concentrations of betaine and choline in the muscle tissue (Table 2) compared to experimental control diet #1, and diets #3, #4 and #5. Relative levels of betaine, choline, glycine, and serine are shown (Figure 7).

Pathway analysis

To determine which metabolic pathways in liver and muscle tissues were the most impacted by the difference in dietary regime between fish fed the natural diet and those fed the experimental soy-based formulations, the metabolites listed in Table 1 and Table 2 were mapped using the Pathway Analysis module implemented in MetaboAnalyst 3.0 software (www.metaboanalyst.ca/MetaboAnalyst). [30] For the analysis, the zebrafish (*Danio rerio*) pathway library was used, and hypergeometric test and relative betweenness centrality algorithms were employed. For each analyzed pathway, a fit coefficient (p) is calculated from pathway enrichment analysis and an impact factor is derived from pathway topology analysis (Figure 8). The glycine, serine and threonine pathway, with the highest value of –log(p) was identified as being the most impacted

pathway both in the liver and muscle, followed by the glycerophospholipid pathway in the liver and amino acid metabolic pathway in the muscle.

From the list of detected metabolites and the signs (positive or negative) of the respective loadings, we can conclude that both lipid catabolism with increased levels of glycerophosphocholine and glycerol 3-phosphate, and protein catabolism with the resulting higher concentrations of free amino acids (mainly alanine, glycine, histidine and serine) are upregulated in red drum fed any of our soy-based experimental formulations, with a generally more pronounced catabolic signature for diet #2. Diet #2 is in fact the soy-formulation among the four evaluated in this study which showed the highest levels of glycerol 3-phosphate and lowest levels of O-phosphocholine in the liver (Figure 6A and 6B and Table 2), and fish fed this diet displayed the highest levels of glycine, serine, 4-hydroxyproline and ATP as well as the lowest levels of betaine and choline in the muscle tissue (Figure 7 and Table 2). These catabolic pathways are important in that they provide precursors for gluconeogenesis. The catabolic pathways that appear to be upregulated in liver and muscle in the soy-based diets show a systematic pattern in liver and muscle (Figure 9). A similar metabolic profile has been described in the literature in the case of prolonged food deprivation in some fish species, such as rainbow trout. [31] It is well known that different fish species normally encounter periods of food deprivation or significant changes in nutritional state over the course of their lives, and therefore their metabolism has adapted to handle possible energy-deficient conditions by differentially relying on lipid, protein and carbohydrate metabolism. The catabolism of stored lipids is known to play a central role in rapid energy production in response to nutritional stress in several fish species, such as salmonids. [32, 33] Protein catabolism on the other hand has

mostly been reported in cases of long-term food deprivation as a secondary energy source, which is mobilized once a low critical level of fat reserves is reached. [31] As far as carbohydrates are concerned, they usually do not represent a major source of energy in fish, due to the absence of carbohydrates in their natural diets. Nevertheless, enzymes responsible for carbohydrate metabolism are present in fish and carbohydrate metabolism has been studied in several fish species especially in response to fasting. The results from these studies indicate that, following an initial depletion of glycogen stores as an early response to food deprivation, as the nutritional stress persists, liver glycogen levels can be replenished, suggesting that the utilization of alternative sources of energy becomes prominent at later stages. [34]

In our study, the analysis of standard growth parameters suggests that red drum can digest and utilize high quantities of different soy protein sources without apparent evidence of starvation or problems related to feed digestibility or absorption of nutrients. Nevertheless, our metabolomics data collectively suggest that red drum fed the soy-based experimental diets investigated in our study are in an energy-deficient state, which is metabolically similar to fasting compared with the natural diet at the metabolic equilibrium established around week 9 in the feeding trial, thus indicating that improvements are still necessary in the composition of soy-based formulations as alternative feeds to fishmeal.

CONCLUSIONS

The present study demonstrates the possibility of evaluating the performance of alternative feeds for aquaculture based on the use of a Nuclear Magnetic Resonance

(NMR) spectroscopy-based metabolomics approach to monitor time-dependent and diet-dependent changes in the fish metabolome. PCA analysis of liver and muscle tissues from red drum at the end-points of the metabolic trajectories shows that there is a significant difference between the natural diet, which mimics what red drum would eat in the wild, and the five formulations of fishmeal-free soy product-containing experimental diets. Further loading plot analysis along with pathway analysis revealed that catabolic pathways related to energy metabolism are upregulated in the soy-based diets compared with the natural diet. These are pathways that provide substrates for gluconeogenesis, via both lipid and protein catabolism, which are overall indicative of a sub-optimal nutritional state characterized by an energetic imbalance for red drum fed any of the soy-based experimental diets used in this study when compared with fish fed the natural diet. Furthermore, despite the fact that few differences in performance were detected based on standard growth parameters among the different soy-based dietary treatments, metabolic differences have been identified both in the liver and in the muscle tissue that allow for the identification of a specific soy formulation, diet #2 as the diet where the catabolic signature is overall more pronounced and the least optimal for red drum production among the experimental diets evaluated in this study.

Disclaimer

Certain commercial equipment, instruments, or materials are identified in this paper to specify adequately the experimental procedure. Such identification does not imply recommendation or endorsement by the National Institute of Standards and Technology, nor does it imply that the materials or equipment identified are necessarily the best

available for the purpose. Reference to the content of this paper for commercial advertising purposes with regard to commercial equipment, instruments, or materials is prohibited (15 CFR 200.113).

ASSOCIATED CONTENT

Supporting Information

Experimental Procedures; **Figures:** Figure S1 – Average weights per time point of red drum fish fed either the soy-based diets or the natural diet. Figure S2 - Liver QC sample PCA score plot. Figure S3 - Muscle QC sample PCA score plot. Figure S4 - Plasma QC sample PCA score plot. Figure S5 - Unsupervised 2D PCA score plots derived from ^{1}H NOESY 1D NMR spectra from red drum muscle tissue. Figure S6 - Unsupervised 2D PCA score plots derived from ^{1}H NOESY 1D NMR spectra from red drum plasma. Figure S7 - Liver PCA score plots for the five soy-based experimental diets (diet #1 to #5) and the natural diet (N) comparing T_0 and T_{end} time points. Figure S8 - Liver T_0-T_{end} PC1 loading plot (95th percentile) for the five experimental diets (diet #1 to diet #5) and the natural diet; **Tables:** Table S1 – Composition of experimental diets for this study. Table S2 - Proximate analyses for whole body. Table S3 - Proximate analyses for fillets. Table S4 - Production characteristics from the feeding trial. Table S5 - Eviscerated fish weight (g) and hepatosomatic index (HSI) at final sampling. Table S6 - Quantiles of % RSD derived from QC sample NMR spectra. Table S7 - Significant metabolites identified in the PCA liver and muscle models for the five experimental diets (diets #1 to #5) and

the natural diet by comparing the T_0 and T_{end} time points. This material is available free of charge via the Internet at http://pubs.acs.org.

AUTHOR INFORMATION

Corresponding Author

*Phone: (843) 762-8865. Fax: (843) 762-8742. E-mail: dan.bearden@nist.gov.

Notes

The authors declare no competing financial interest.

AKNOWLEDGMENTS

We thank SCDNR personnel Andrew Grosse, Mata McAskill, Matt Perkinson, Chris Katalinas, Katie Anweiler, Tim O'Donnell, Maggie Jamison, David Flanagan and Rachel Buissereth for their assistance with fish tissue sampling. Rachel Buissereth was supported by NSF REU Site: Research Experience for Undergraduate Minorities in Marine and Environmental Sciences grant #126280. We acknowledge the Soy Aquaculture Alliance and the United Soybean Board for funding support of this research. This is contribution number xxx (To Be Determined on acceptance for publication) from the South Carolina Department of Natural Resources Marine Resources Research Institute.

REFERENCES

(1) The State of World Fisheries and Aquaculture. *Rome: Food and Agriculture Organization of the United Nations* **2014**.

(2) Naylor, R. L.; Goldburg, R. J.; Primavera, J. H.; Kautsky, N.; Beveridge, M. C.; Clay, J.; Folke, C.; Lubchenco, J.; Mooney, H.; Troell, M. Effect of aquaculture on world fish supplies. *Nature* **2000,** *405*, 1017-1024.

(3) Gaylord, T. G.; Gatlin III, D. M. Determination of digestibility coefficients of various feedstuffs for red drum (Sciaenops ocellatus). *Aquaculture* **1996,** *139*, 303-314.

(4) McGoogan, B. B.; Reigh, R. C. Apparent digestibility of selected ingredients in red drum (Sciaenops ocellatus) diets. *Aquaculture* **1996,** *141*, 233-244.

(5) McGoogan, B. B.; Gatlin, D. M. Effects of Replacing Fish Meal with Soybean Meal in Diets for Red Drum Sciaenops ocellatus and Potential for Palatability Enhancement. *J. World Aquacult. Soc.* **1997,** *28*, 374-385.

(6) Davis, D. A.; Miller, C. L.; Phelps, R. P. Replacement of Fish Meal with Soybean Meal in the Production Diets of Juvenile Red Snapper, Lutjanus campechanus. *J. World Aquacult. Soc.* **2005,** *36*, 114-119.

(7) Schock, T. B.; Newton, S.; Brenkert, K.; Leffler, J.; Bearden, D. W. An NMR-based metabolomic assessment of cultured cobia health in response to dietary manipulation. *Food Chem.* **2012,** *133*, 90-101.

(8) Yaghoubi, M.; Mozanzadeh, M. T.; Marammazi, J. G.; Safari, O.; Gisbert, E. Dietary replacement of fish meal by soy products (soybean meal and isolated soy protein) in silvery-black porgy juveniles (Sparidentex hasta). *Aquaculture* **2016,** *464*, 50-59.

(9) Buentello, A.; Jirsa, D.; Barrows, F. T.; Drawbridge, M. Minimizing fishmeal use in juvenile California yellowtail, Seriola lalandi, diets using non-GM soybeans selectively bred for aquafeeds. *Aquaculture* **2015,** *435*, 403-411.

(10) Gatlin, D. M.; Barrows, F. T.; Brown, P.; Dabrowski, K.; Gaylord, T. G.; Hardy, R. W.; Herman, E.; Hu, G.; Krogdahl, Å.; Nelson, R.; Overturf, K.; Rust, M.; Sealey, W.; Skonberg, D.; J Souza, E.; Stone, D.; Wilson, R.; Wurtele, E. Expanding the utilization of sustainable plant products in aquafeeds: a review. *Aquacult. Res.* **2007,** *38*, 551-579.

(11) Francis, G.; Makkar, H. P. S.; Becker, K. Antinutritional factors present in plant-derived alternate fish feed ingredients and their effects in fish. *Aquaculture* **2001,** *199*, 197-227.

(12) Moon, H. Y.; Gatlin, D. M. Total sulfur amino acid requirement of juvenile red drum, Sciaenops ocellatus. *Aquaculture* **1991,** *95*, 97-106.

(13) Craig, S. R.; Gatlin, D. M. Dietary Lysine Requirement of Juvenile Red Drum Sciaenops ocellatus. *J. World Aquacult. Soc.* **1992,** *23*, 133-137.

(14) McGoogan, B. B.; Gatlin, D. M., 3rd Metabolic requirements of red drum, Sciaenops ocellatus, for protein and energy based on weight gain and body composition. *J. Nutr.* **1998,** *128*, 123-129.

(15) Viant, M. R. Metabolomics of aquatic organisms: the new 'omics' on the block. *Mar. Ecol.: Prog. Ser.* **2007,** *332*, 301.

(16) Bearden, D. W. Environmental Metabolomics. *eMagRes* **2012,** *1*, 1-12.

(17) Viant, M. R.; Werner, I.; Rosenblum, E. S.; Gantner, A. S.; Tjeerdema, R. S.; Johnson, M. L. Correlation between heat-shock protein induction and reduced metabolic condition in juvenile steelhead trout (Oncorhynchus mykiss) chronically exposed to elevated temperature. *Fish Physiol. Biochem.* **2003,** *29*, 159-171.

(18) Viant, M. R.; Rosenblum, E. S.; Tieerdema, R. S. NMR-based metabolomics: a powerful approach for characterizing the effects of environmental stressors on organism health. *Environ. Sci. Technol.* **2003,** *37*, 4982-4989.

(19) Viant, M. R.; Bearden, D. W.; Bundy, J. G.; Burton, I. W.; Collette, T. W.; Ekman, D. R.; Ezernieks, V.; Karakach, T. K.; Lin, C. Y.; Rochfort, S.; Ropp, J. S. d.; Teng, Q.; Tjeerdema, R. S.; Walter, J. A.; Wu, H. International NMR-Based Environmental Metabolomics Intercomparison Exercise. *Environ. Sci. Technol.* **2009,** *43*, 219-225.

(20) Bligh, E. G.; Dyer, W. J. A rapid method of total lipid extraction and purification. *Can. J. Biochem. Physiol.* **1959,** *37*, 911-917.

(21) Lin, C. Y.; Wu, H.; Tjeerdema, R. S.; Viant, M. R. Evaluation of metabolite extraction strategies from tissue samples using NMR metabolomics. *Metabolomics* **2007,** *3*, 55-67.

(22) Viant, M. R. Revealing the metabolome of animal tissues using 1H nuclear magnetic resonance spectroscopy. *Methods Mol. Biol. (N. Y., NY, U. S.)* **2007,** *358*, 229-246.

(23) Schock, T. B.; Duke, J.; Goodson, A.; Weldon, D.; Brunson, J.; Leffler, J. W.; Bearden, D. W. Evaluation of Pacific White Shrimp (Litopenaeus vannamei) Health during a Superintensive Aquaculture Growout Using NMR-Based Metabolomics. *PLoS One* **2013,** *8*, e59521.

(24) Ludwig, C.; Easton, J. M.; Lodi, A.; Tiziani, S.; Manzoor, S. E.; Southam, A. D.; Byrne, J. J.; Bishop, L. M.; He, S.; Arvanitis, T. N.; Günther, U. L.; Viant, M. R. Birmingham Metabolite Library: a publicly accessible database of 1-D 1H and 2-D 1H J-resolved NMR spectra of authentic metabolite standards (BML-NMR). *Metabolomics* **2012,** *8*, 8-18.

(25) Nicholson, J. K.; Foxall, P. J.; Spraul, M.; Farrant, R. D.; Lindon, J. C. 750 MHz 1H and 1H-13C NMR spectroscopy of human blood plasma. *Anal. Chem.* **1995,** *67*, 793-811.

(26) Wishart, D. S.; Jewison, T.; Guo, A. C.; Wilson, M.; Knox, C.; Liu, Y.; Djoumbou, Y.; Mandal, R.; Aziat, F.; Dong, E.; Bouatra, S.; Sinelnikov, I.; Arndt, D.; Xia, J.; Liu, P.; Yallou, F.; Bjorndahl, T.; Perez-Pineiro, R.; Eisner, R.; Allen, F.; Neveu, V.; Greiner, R.; Scalbert, A. HMDB 3.0--The Human Metabolome Database in 2013. *Nucleic Acids Res*. **2012,** *41*, D801-807.

(27) Ulrich, E. L.; Akutsu, H.; Doreleijers, J. F.; Harano, Y.; Ioannidis, Y. E.; Lin, J.; Livny, M.; Mading, S.; Maziuk, D.; Miller, Z.; Nakatani, E.; Schulte, C. F.; Tolmie, D. E.; Kent Wenger, R.; Yao, H.; Markley, J. L. BioMagResBank. *Nucleic Acids Res*. **2008,** *36*, D402-408.

(28) Sumner, L.; Amberg, A.; Barrett, D.; Beale, M.; Beger, R.; Daykin, C.; Fan, T. M.; Fiehn, O.; Goodacre, R.; Griffin, J.; Hankemeier, T.; Hardy, N.; Harnly, J.; Higashi, R.; Kopka, J.; Lane, A.; Lindon, J.; Marriott, P.; Nicholls, A.; Reily, M.; Thaden, J.; Viant, M. Proposed minimum reporting standards for chemical analysis. *Metabolomics* **2007,** *3*, 211-221.

(29) Parsons, H. M.; Ekman, D. R.; Collette, T. W.; Viant, M. R. Spectral relative standard deviation: a practical benchmark in metabolomics. *Analyst* **2009,** *134*, 478-485.

(30) Xia, J.; Sinelnikov, I. V.; Han, B.; Wishart, D. S. MetaboAnalyst 3.0--making metabolomics more meaningful. *Nucleic Acids Res*. **2015,** *43*, W251-257.

(31) Kullgren, A.; Samuelsson, L. M.; Larsson, D. G.; Bjornsson, B. T.; Bergman, E. J. A metabolomics approach to elucidate effects of food deprivation in juvenile rainbow

trout (Oncorhynchus mykiss). *Am. J. Physiol.: Regul., Integr. Comp. Physiol.* **2010,** *299*, R1440-1448.

(32) Farbridge, K. J.; Leatherland, J. F. Temporal changes in plasma thyroid hormone, growth hormone and free fatty acid concentrations, and hepatic 5'-monodeiodinase activity, lipid and protein content during chronic fasting and re-feeding in rainbow trout (Oncorhynchus mykiss). *Fish Physiol. Biochem.* **1992,** *10*, 245-257.

(33) Navarro, I.; Gutierrez, J.; Planas, J. Changes in plasma glucagon, insulin and tissue metabolites associated with prolonged fasting in brown trout (Salmo trutta fario) during two different seasons of the year. *Comp. Biochem. Physiol., A: Comp. Physiol.* **1992,** *102*, 401-407.

(34) Sheridan, M. A.; Mommsen, T. P. Effects of nutritional state on in vivo lipid and carbohydrate metabolism of coho salmon, Oncorhynchus kisutch. *Gen. Comp. Endocrinol.* **1991,** *81*, 473-483.

Table 1. Metabolites identified in the liver and muscle PCA models that were found to be significantly different between the soy-based experimental diets (diet #1 to diet #5) and the natural diet at T_{end}. Metabolite identity was confirmed using ^{1}H, 2D JRES and ^{1}H, ^{13}C HSQC spectra. Fold change is calculated by the average bin intensities of metabolites in soy-based diet samples (average value for diets #2 to diet #5) divided by the average bin intensities of natural diet samples. Values are all statistically significant (Wilcoxon test; $P < 0.0001$).

Table 1. (Continued)

Metabolites	^{1}H and ^{13}C Chemical shift (ppm), multiplicities and J_{HH} couplings (Hz)	Fold change (over natural diet)	Tissue
Alanine	(1.48 (d, J = 7.2 Hz), 19.0), (3.78 (q, J = 7.2 Hz), 53.3)	1.43 (L), 1.75 (M)	L, M
ATP	(4.24 (m), 67.9), (4.29 (m), 67.9), (4.41 (m), 86.8), (4.60, 72.9), (4.81, 77.1), (6.15 (d, J = 4.8 Hz), 89.6), (8.27 (s), 155.5), (8.54 (s), 142.8)	1.45	M
Beta-alanine	(2.56 (t, J = 6.7 Hz), 36.4), (3.18 (t, J = 6.7 Hz), 39.3)	1.44	L
Betaine	(3.27 (s), 56.2), (3.91(s), 69.0)	0.75	M
Carnitine	(2.44 (m), 45.7), (2.46 (m), 45.9), (3.23 (s), 56.9), (3.43(m), 72.9)	2.11	M
Creatine	(3.04 (s), 39.7), (3.93 (s), 56.7)	1.35	M
Creatine phosphate	(3.04 (s), 39.5), (3.95 (s), 56.7)		M
Dimethylglycine	(2.93 (s), 46.3)	0.08	L
Glucose	(3.25 (dd, J_1 = 9.3 Hz, J_2 = 7.9 Hz), 77.0), (3.41 (m), 72.5), (3.46 (m), 78.7), (3.48 (t, J = 9.3 Hz), 78.7), (3.54, (dd, J_1 = 10.0 Hz, J_2 = 3.9 Hz), 74.3), (3.72 (m), 75.6), (3.72 (m), 63.6), (3.78 (dd, J_1 = 14.4, J_2 = 7.0 Hz), 63.4), (3.84 (m),74.3), (3.84 (m), 63.4), (3.90 (dd, J_1 = 12.4 Hz, J_2 = 2.4 Hz), 63.6), (4.65 (d, J = 7.7 Hz), 98.8), (5.24 (d, J = 3.8 Hz), 94.9)	0.62	L
Glutathione	(2.17 (m), 29.0), (2.56 (m), 34.2), (2.96 (m), 28.3), (3.30, 41.6), (3.32, 41.6), (3.78 (m), 46.2), (3.79 (m), 57.0), (4.57 (dd, J_1 = 7.3 Hz, J_2 = 5.1 Hz), 58.6), (4.76, 55.5)	0.31	L
Glycerol 3-phosphate	(3.62 (dd, J_1 = 11.6 Hz, J_2 = 5.9 Hz), 65.0), (3.68 (dd, J_1 = 11.5 Hz, J_2 = 4.7 Hz), 65.1), (3.78 (m), 73.9), (3.80 (m), 67.7), (3.83 (m), 67.7), (3.84 (m), 74.0), (3.88 (m), 74.0), (3.89 (m), 74.0)	1.44	L
Glycerophosphocholine	(3.23 (s), 56.9), (3.62 (dd, J_1 = 11.9 Hz, J_2 = 5.8 Hz), 64.6), (3.68 (m), 64.7), (3.69 (dd, J_1 = 11.5 Hz, J_2 = 4.6 Hz), 68.8), (3.89 (m), 69.4), (3.90 (m), 73.5), (3.94 (m), 69.3), (4.33 (m), 62.2)	1.63	L
Glycine	(3.56 (s), 44.2)	2.46 (L), 8.72 (M)	L, M
Glycogen	(3.47 (m), 72.4), (3.66 (m), 79.7), (3.77 (m), 75.8), (3.87 (m), 63.3), (3.96 (dd, J_1 = 10.0 Hz, J_2 = 8.6 Hz), 76.1), (3.98 (dd, J_1 = 10.8 Hz, J_2 = 8.5 Hz), 76.1), (5.40 (d, J = 3.8 Hz), 102.4), (5.41 (d, J = 4.5 Hz), 102.4)	1.69	L
Histidine	(3.15 (ddd, J_1 = 15.4 Hz, J_2 = 7.7 Hz, J_3 = 1.1 Hz), 30.7), (3.25 (ddd, J_1 = 15.4 Hz, J_2 = 4.7 Hz, J_3 = 1.6 Hz), 30.8), (3.99 (dd, J_1 = 7.8, J_2 = 4.7 Hz), 57.5), (7.09 (d, J = 1.4 Hz), 119.6), (7.88 (d, J = 1.4 Hz), 138.5)	1.79	M
4-Hydroxyproline	(2.15 (m), 40.2), (2.44 (m), 40.2), (3.37 (t, J = 1.9 Hz), 55.7), (3.38 (t, J = 1.9 Hz), 55.7), (3.48 (dd, J_1 = 11.5 Hz, J_2 = 3.8 Hz), 55.8), (3.50 (dd, J_1 = 12.4 Hz, J_2 = 3.6 Hz), 55.8), (4.35 (ddd, J_1 = 10.8 Hz, J_2 = 7.7 Hz, J_3 = 1.1 Hz), 62.6), (4.67 (m), 72.9)	2.35	M
Lactate	(1.33 (d, J = 7.0 Hz), 22.8), (4.11 (q, J = 7.0 Hz), 71.3)	0.93	L
Lysine	(1.46 (m), 24.5), (1.51 (m), 24.4), (1.73 (m), 29.3), (1.91 (m), 32.6), (3.03 (t, J = 7.9 Hz), 42.0), (3.76 (t, J = 5.8 Hz), 57.4)	0.24	M
Malate	(2.35 (dd, J_1 = 15.4 Hz, J_2 = 10.2 Hz), 45.5), (2.67 (dd, J_1 = 15.4 Hz, J_2 = 3.1 Hz), 45.5), (4.30 (dd, J_1 = 10.2 Hz, J_2 = 3.1 Hz), 73.2)	2.56	M
Malonate	(3.11 (s), 48.7)	0.13	L
Maltose	(3.23, 56.9), (3.28, 77.0), (3.43, 72.6), (3.58, 74.3), (3.60, 77.4), (3.65, 79.5), (3.72, 75.3), (3.75, 63.4), (3.78, 79.0), (3.80, 63.3), (3.84, 63.3), (3.90, 63.4), (3.94 (m), 72.8), (3.98 (t, J = 9.1 Hz), 76.0), (4.64 (d), 98.6), (5.24 (d), 94.8), (5.42 (d, J = 3.8 Hz), 102.3)	1.44	L
Ornithine	(1.75 (m), 25.6), (1.77 (m), 25.6), (1.84 (m), 25.6), (1.85 (m), 25.7), (1.94 (m), 30.3), (3.05 (t, J = 7.8 Hz), 41.6)	0.23	M
O-phosphocholine	(3.22 (s), 56.8), (3.59 (m), 69.3), (4.17 (m), 60.8)	0.59	L
Sarcosine	(2.74 (s), 35.5), (3.61 (s), 53.6)	0.10	L
Serine	(3.85 (dd, J_1 = 5.7 Hz, J_2 = 3.5 Hz), 59.2), (3.97 (m), 63.0)	1.28	M
Succinate	(2.41 (s), 37.0)	0.51	L
Taurine	(3.27 (t, J = 6.7 Hz), 50.4), (3.42 (t, J = 6.7 Hz), 38.1)	1.42 (L), 1.41 (M)	L, M
Threonine	(1.33 (d, J = 6.9 Hz), 22.5), (3.59 (d, J = 5.3 Hz), 63.3), (4.25 (m), 68.8)	0.74	L
TMAO	(3.27 (s), 62.4)	0.22	M
Unknown_dwb_04	(3.30 (s), 55.0)		L
Unknown_fc_105	(3.39 (s), 57.4)		L
Unknown_fc_106	(3.20 (s), 54.1)		L
Unknown_fc_107	(3.14 (s), 55.7)		L
Unknown_fc_108	(4.53 (s), 77.9)		L
Unknown_fc_121	(2.79 (s), 35.9)		L
Unknown_fc_122	(2.72 (s), 34.6)		L

Chemical shifts were referenced to the internal standard TMSP $\delta^{1}H$ 0.00. Key: s, singlet; d, doublet; dd, doublet of doublets; t, triplet; m, multiplet. TMAO, trimethylamine-*N*-oxide. L, Liver; M, Muscle. Underlined chemical shifts indicate well-isolated signals used in metabolite level determination via bin intensities.

Table 2. Metabolites identified in the PCA liver and muscle models that were found to be significantly different among the soy-based experimental diets (diet #1 to diet #5). The natural diet was not included. Compound identity was confirmed using ^{1}H, 2D JRES and ^{1}H, ^{13}C HSQC spectra. Fold change is calculated by the average bin intensities of metabolites in soy-based diet #2 to diet #5 divided by the average bin intensities of diet #1 samples (control). Values not sharing the same superscripts are significantly different ($P < 0.05$) based on Tukey's test).

Table 2. (Continued)

Metabolites	^{1}H and ^{13}C Chemical shift (ppm), multiplicities and J_{HH} couplings (Hz)	Fold change (over Diet 1 - SBM60)				Tissue
		Diet 2	Diet 3	Diet 4	Diet 5	
Alanine	(1.48 (d, J = 7.2 Hz), 19.0), (3.78 (q, J = 7.2 Hz), 53.3)	1.14^{ab}	1.18^{a}	0.91^{c}	1.08^{ab}	L
Anserine	(2.67 (m), 34.8), (2.70 (m), 34.8), (3.04, 28.9), (3.21 (m), 38.4), (3.22 (m), 28.9), (3.24 (m), 28.8), (3.77 (s), 35.1), (4.49 (m), 56.2), (7.06 (d, J = 1.4 Hz), 124.0), (8.15 (s, broad), 140.0)	1.08^{a}	0.87^{b}	0.97^{ab}	0.90^{b}	M
Asparagine	(2.86 (dd, J1 = 16.6 Hz, J2 = 7.4 Hz), 37.5), (2.96 (dd, J1 = 16.6 Hz, J2 = 4.2 Hz), 37.5), (4.00 (dd, J1 = 7.7 Hz, J2 = 4.6 Hz), 54.1)	0.97^{ab}	0.95^{ab}	0.80^{bc}	0.74^{c}	M
ATP	(4.24 (m), 67.9), (4.29 (m), 67.9), (4.41 (m), 86.8), (4.60, 72.9), (4.81, 77.1), (6.15 (d, J = 4.8 Hz), 89.6), (8.27 (s), 155.5), (8.54 (s), 142.8)	1.13^{a}	1.05^{b}	1.03^{b}	1.02^{b}	M
Betaine	(3.27 (s), 56.2), (3.91(s), 69.0)	0.32^{a}	0.68^{b}	1.05^{c}	1.07^{c}	M
Carnitine	(2.44 (m), 45.7), (2.46 (m), 45.9), (3.23 (s), 56.9), (3.43(m), 72.9)	1.08^{a}	1.01^{ab}	0.98^{ab}	0.96^{b}	M
Choline	(3.21 (s), 56.6), (3.52 (m), 70.3), (4.07 (m), 58.4)	0.60^{a}	0.84^{b}	1.02^{c}	1.05^{c}	M
Glucose	(3.25 (dd, J_1 = 9.3 Hz, J_2 = 7.9 Hz), 77.0), (3.41 (m), 72.5), (3.46 (m), 78.7), (3.48 (t, J = 9.3 Hz), 78.7), (3.54, (dd, J_1 = 10.0 Hz, J_2 = 3.9 Hz), 74.3), (3.72 (m), 75.6), (3.72 (m), 63.6), (3.78 (dd, J_1 = 14.4, J_2 = 7.0 Hz), 63.4), (3.84 (m),74.3), (3.84 (m), 63.4), (3.90 (dd, J_1 = 12.4 Hz, J_2 = 2.4 Hz), 63.6), (4.65 (d, J = 7.7 Hz), 98.8), (5.24 (d, J = 3.8 Hz), 94.9)	1.03^{a}	0.89^{b}	1.01^{ab}	1.00^{ab}	L
Glutamate	(2.06 (m), 29.8), (2.13 (m), 29.8), (2.35 (m), 36.3), (3.76 (dd, J1 = 6.9 Hz, J2 = 4.7 Hz), 57.4)	0.86^{a}	1.00^{b}	0.97^{ab}	0.88^{a}	L
Glutamine	(2.15 (m), 29.1), (2.46 (m), 33.7), (3.78 (t, J = 6.3 Hz), 57.0)	0.80^{a}	1.09^{b}	0.84^{a}	1.18^{b}	L
Glutathione	(2.17 (m), 29.0), (2.56 (m), 34.2), (2.96 (m), 28.3), (3.30, 41.6), (3.32, 41.6), (3.78 (m), 46.2), (3.79 (m), 57.0), (4.57 (dd, J_1 = 7.3 Hz, J_2 = 5.1 Hz), 58.6), (4.76, 55.5)	0.86^{a}	0.91^{ab}	0.90^{ab}	0.91^{ab}	L
Glycerol 3-phosphate	(3.62 (dd, J_1 = 11.6 Hz, J_2 = 5.9 Hz), 65.0), (3.68 (dd, J_1 = 11.5 Hz, J_2 = 4.7 Hz), 65.1), (3.78 (m), 73.9), (3.80 (m), 67.7), (3.83 (m), 67.7), (3.84 (m), 74.0), (3.88 (m), 74.0), (3.89 (m), 74.0)	1.28^{a}	1.09^{b}	1.05^{b}	1.04^{b}	L
Glycine	(3.56 (s), 44.2)	1.32^{a}	1.02^{b}	1.05^{b}	1.04^{b}	M
Glycogen	(3.47 (m), 72.4), (3.66 (m), 79.7), (3.77 (m), 75.8), (3.87 (m), 63.3), (3.96 (dd, J_1 = 10.0 Hz, J_2 = 8.6 Hz), 76.1), (3.98 (dd, J_1 = 10.8 Hz, J_2 = 8.5 Hz), 76.1), (5.40 (d, J = 3.8 Hz), 102.4), (5.41 (d, J = 4.5 Hz), 102.4)					L
Histidine	(3.15 (ddd, J_1 = 15.4 Hz, J_2 = 7.7 Hz, J_3 = 1.1 Hz), 30.7), (3.25 (ddd, J_1 = 15.4 Hz, J_2 = 4.7 Hz, J_3 = 1.6 Hz), 30.8), (3.99 (dd, J_1 = 7.8, J_2 = 4.7 Hz), 57.5), (7.09 (d, J = 1.4 Hz), 119.6), (7.88 (d, J = 1.4 Hz), 138.5)	1.06^{a}	0.80^{b}	0.95^{ab}	0.82^{b}	M
4-Hydroxyproline	(2.15 (m), 40.2), (2.44 (m), 40.2), (3.37 (t, J = 1.9 Hz), 55.7), (3.38 (t, J = 1.9 Hz), 55.7), (3.48 (dd, J_1 = 11.5 Hz, J_2 = 3.8 Hz), 55.8), (3.50 (dd, J_1 = 12.4 Hz, J_2 = 3.6 Hz), 55.8), (4.35 (ddd, J_1 = 10.8 Hz, J_2 = 7.7 Hz, J3 = 1.1 Hz), 62.6), (4.67 (m), 72.9)	1.10^{a}	0.94^{b}	0.92^{b}	0.87^{b}	M
Lactate	(1.33 (d, J = 7.0 Hz), 22.8), (4.11 (q, J = 7.0 Hz), 71.3)	1.16^{a}	1.12^{a}	0.94^{b}	1.16^{a}	M
Maltose	(3.23, 56.9), (3.28, 77.0), (3.43, 72.6), (3.58, 74.3), (3.60, 77.4), (3.65, 79.5), (3.72, 75.3), (3.75, 63.4), (3.78, 79.0), (3.80, 63.3), (3.84, 63.3), (3.90, 63.4), (3.94 (m), 72.8), (3.98 (t, J = 9.1 Hz), 76.0), (4.64 (d), 98.6), (5.24 (d), 94.8), (5.42 (d, 3.8 Hz), 102.3)					L
O-phosphocholine	(3.22 (s), 56.8), (3.59 (m), 69.3), (4.17 (m), 60.8)	0.64^{a}	0.92^{bc}	1.06^{d}	0.86^{b}	L
Proline	(2.01 (m), 26.6), (2.08 (m), 31.8), (2.35 (m), 31.8), (3.34 (m), 48.9), (3.42, 48.8), (4.14 (dd, J1 = 8.1 Hz, J2 = 5.8 Hz), 64.0)	0.88^{ab}	0.77^{b}	0.79^{ab}	0.73^{b}	M
Serine	(3.85 (dd, J_1 = 5.7 Hz, J_2 = 3.5 Hz), 59.2), (3.97 (m), 63.0)	1.42^{a}	1.10^{b}	0.89^{b}	1.02^{b}	M
Taurine	(3.27 (t, J = 6.7 Hz), 50.4), (3.42 (t, J = 6.7 Hz), 38.1)	0.86^{a}	1.10^{b}	1.01^{ab}	0.95^{ab}	M
Threonine	(1.33 (d, J = 6.9 Hz), 22.5), (3.59 (d, J = 5.3 Hz), 63.3), (4.25 (m), 68.8)					M

Chemical shifts were referenced to the internal standard TMSP δ1H 0.00. Key: s, singlet; d, doublet; dd, doublet of doublets; t, triplet; m, multiplet. L, Liver; M, Muscle. Underlined chemical shifts indicate well-isolated signals used in metabolite level determination via bin intensities. Values with different superscript letters are significantly different from each other.

Figure Legends

Figure 1. Unsupervised PCA score plots derived from ^{1}H NOESY 1D NMR spectra from red drum liver tissue (independent models). A) Natural diet; B) diet #1 (SBM60); C) diet #2; D) diet #3; E) diet #4; F) diet #5. Sampled time points were T_0 (n = 63) for sampling at the end of the conditioning period, T_2 to T_5 and T_9 to T_{12} (n = 12/time point) for sampling at weeks 2 to week 5 and week 9 to week 12, respectively. Error bars represent the mean ± 1 SEM.

Figure 2. Unsupervised PCA score plots (independent models) from (A) liver tissue and (B) muscle tissue for the five soy-based experimental diets (diet #1 to diet #5) at the end-point (T_{end}) of the metabolic trajectory including the natural diet (N). For comparison, recalculated PCA score plots for (C) liver and (D) muscle exclude the natural diet (N). Error bars represent the mean ± 1 SEM. Sample numbers are: diet #1 (n = 44, liver; n = 47, muscle), diet #2 (n = 44, liver; n = 46, muscle), diet #3 (n = 46, liver; n = 48, muscle), diet #4 (n = 47, liver; n = 48, muscle), diet #5 (n = 47, liver; n = 48, muscle), natural diet (n = 47, liver; n = 48, muscle).

Figure 3. (A) Liver end-point (T_{end}) PC1 loading plot (95th percentile) for the five experimental diets (diet #1-#5) compared with the natural diet. (B) Expansion of the PC1 loading plot in (A). (C) Liver end-point (T_{end}) PC1 loading plot (95th percentile) for the five experimental diets (diet #1 to #5) excluding the natural diet. (D) Expansion of the

PC1 loading plot in (C). Assignment information is shown in Tables 1 and 2. Glycero-PC, glycerophosphocholine; glycerol 3-P, glycerol 3-phosphate. (A and B) Loadings with a negative sign indicate metabolites that are present at lower levels in the soy-based diets and higher in the natural diet and vice versa. (C and D) Loadings with a negative sign indicate metabolites that are present at higher levels in diets #1, #3, #4 and #5 and lower in diet #2 and vice versa. The horizontal axis represents NMR chemical shift in ppm.

Figure 4. Profile of significantly altered metabolites identified in soy-based diets compared to natural diet for red drum (A) liver tissue and (B) muscle tissue at T_{end}. Glycero-PC, glycerophosphocholine; glycerol 3-P, glycerol 3-phosphate; TMAO, trimethylamine-*N*-oxide. The histograms represent fold change, which is calculated by the average bin intensities of metabolite in soy-based diet samples (average value for diets #2 to #5) divided by the average bin intensities of natural diet samples. Error bars represent mean ± SD (n = 5).

Figure 5. (A) Muscle end-point (T_{end}) PC1 loading plot (95^{th} percentile) for the five experimental diets (diets #1 – diet #5) compared with the natural diet. (B) Expansion of the PC1 loading plot in (A). (C) Muscle end-point (T_{end}) PC1 loading plot (95^{th} percentile) for the five experimental diets (diet #1 to #5) excluding the natural diet. (D). Expansion of the PC1 loading plot in (C). Assignment information is shown in Tables 1 and 2. TMAO, trimethylamine-*N*-oxide. (A and B) Loadings with a negative sign indicate metabolites that are present at lower levels in the soy-based diets and higher in the natural

diet and vice versa. (C and D) Loadings with a negative sign indicate metabolites that are present at higher levels in diets #1, #3, #4 and #5 and lower in diet #2 and vice versa. The horizontal axis represents NMR chemical shift in ppm.

Figure 6. Levels of A) glycerol 3-phosphate and B) O-phosphocholine in soy-based diets from red drum liver tissue at T_{end}. The natural diet was not included. The histograms represent bin intensities. Error bars represent mean ± 1 SEM. *** indicate statistical significance level for $P < 0.001$ (one-way ANOVA with Tukey post-hoc test; $n = 44$ to 47 samples for each dietary treatment as indicated).

Figure 7. Levels of A) betaine, B) choline, C) glycine and D) serine in soy-based diets (diet #1 to #5) from red drum muscle tissue at T_{end}. The natural diet was not included. The histograms represent bin intensities. Error bars represent mean ± 1 SEM. Statistical significance levels for diet #2 are illustrated as * for $P < 0.05$, ** for $P < 0.01$, and *** for $P < 0.001$ (one-way ANOVA with Tukey post-hoc test; $n = 46$ to 48 samples for each dietary treatment as indicated).

Figure 8. Metabolomics pathway analysis overview for A) liver tissue and B) muscle tissue indicating the metabolic pathways that are mostly affected by the different dietary regimes (natural diet and soy-based formulations). The diameter of the circles (nodes)

indicates the pathway impact; the color of the nodes is graded from white to red with increasing *P*-value derived from enrichment analysis.

Figure 9. Overview of the general metabolic network related to energy metabolism affected by the different diets. Red arrows indicate the general pathways that appear to be upregulated in red drum fed any of the experimental soy-based diets compared with the natural diet.

Figure 1.

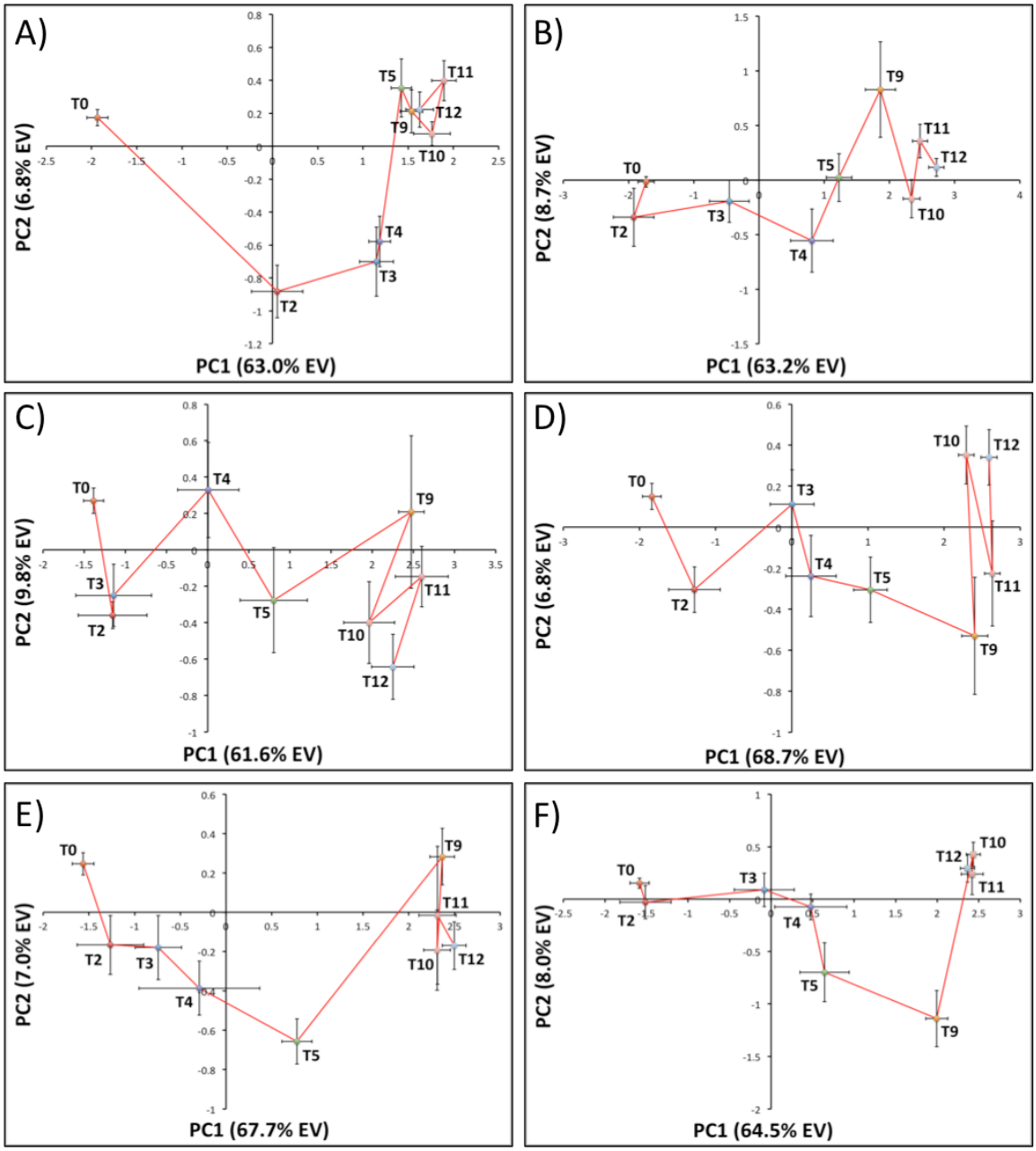
A)
PC2 (6.8% EV)
PC1 (63.0% EV)
T0
T2
T3
T4
T5
T9
T10
T11
T12
B)
PC2 (8.7% EV)
PC1 (63.2% EV)
C)
PC2 (9.8% EV)
PC1 (61.6% EV)
D)
PC2 (6.8% EV)
PC1 (68.7% EV)
E)
PC2 (7.0% EV)
PC1 (67.7% EV)
F)
PC2 (8.0% EV)
PC1 (64.5% EV)

Figure 2.

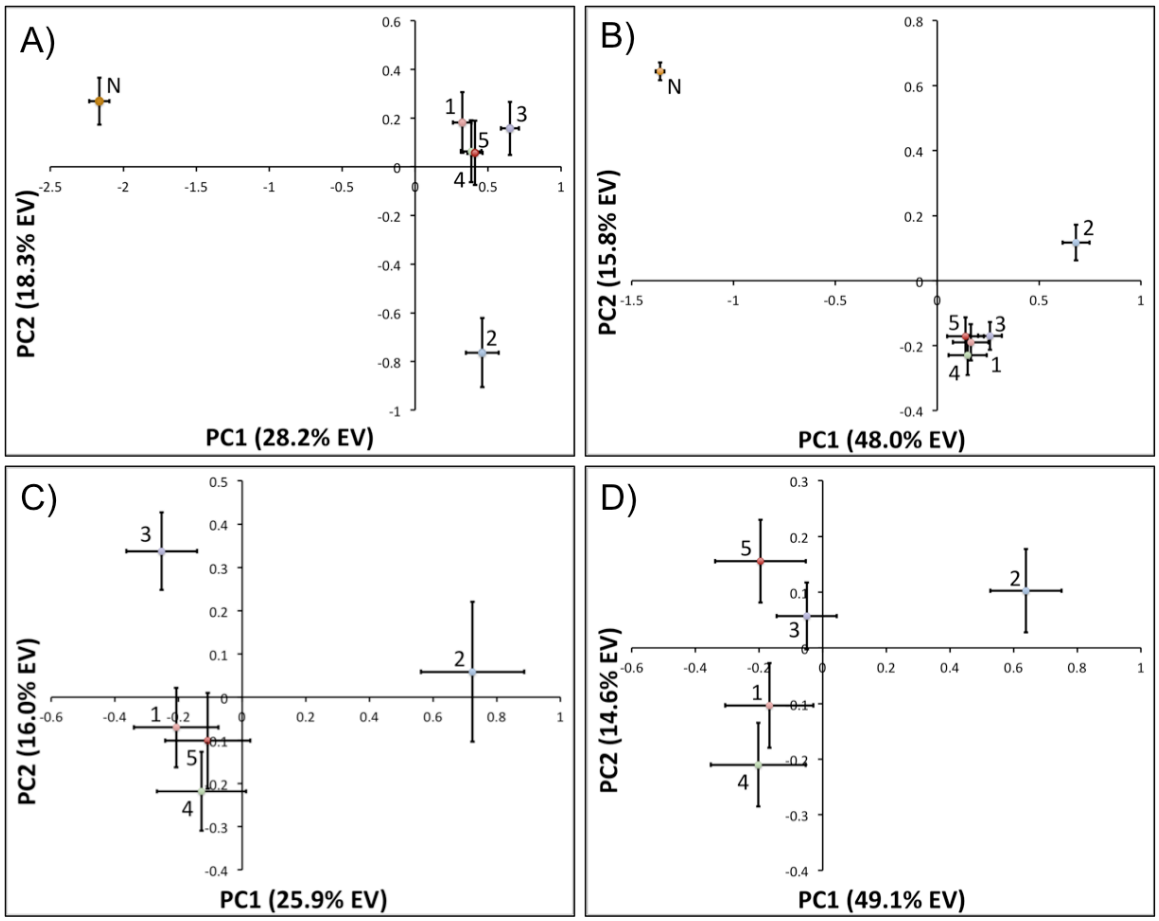
A)
N
1
2
3
4
5
PC2 (18.3% EV)
PC1 (28.2% EV)
B)
N
1
2
3
4
5
PC2 (15.8% EV)
PC1 (48.0% EV)
C)
1
2
3
4
5
PC2 (16.0% EV)
PC1 (25.9% EV)
D)
1
2
3
4
5
PC2 (14.6% EV)
PC1 (49.1% EV)

Figure 3.

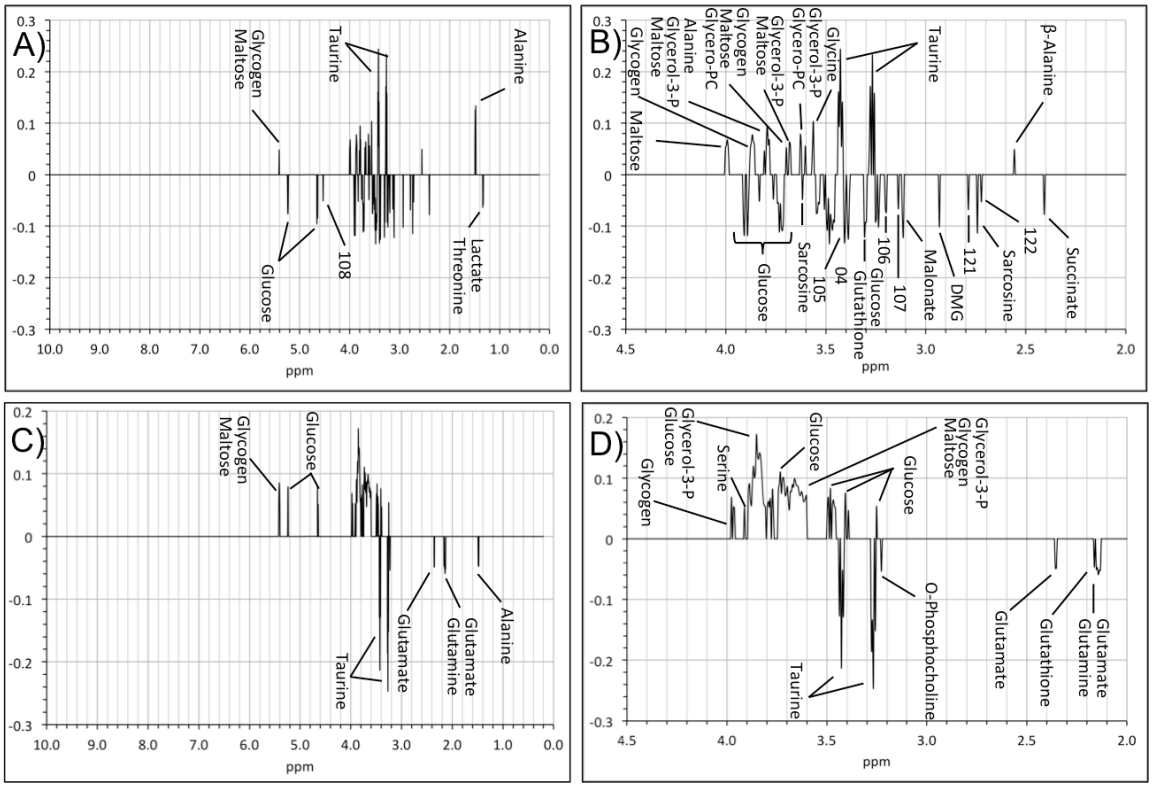
A)
Glycogen
Maltose
Taurine
Alanine
Glucose
108
Lactate
Threonine
B)
Glycogen
Maltose
Alanine
Glycerol-3-P
Glycero-PC
Glycine
Taurine
β-Alanine
Glucose
Sarcosine
105
04
Glucose
Glutathione
106
107
Malonate
DMG
121
Sarcosine
122
Succinate
C)
Glycogen
Maltose
Glucose
Taurine
Glutamate
Glutamine
Alanine
D)
Glycogen
Glucose
Glycerol-3-P
Serine
Glucose
Glycogen
Maltose
Glucose
Taurine
O-Phosphocholine
Glutamate
Glutathione
Glutamine
Glutamate
ppm

Figure 4.

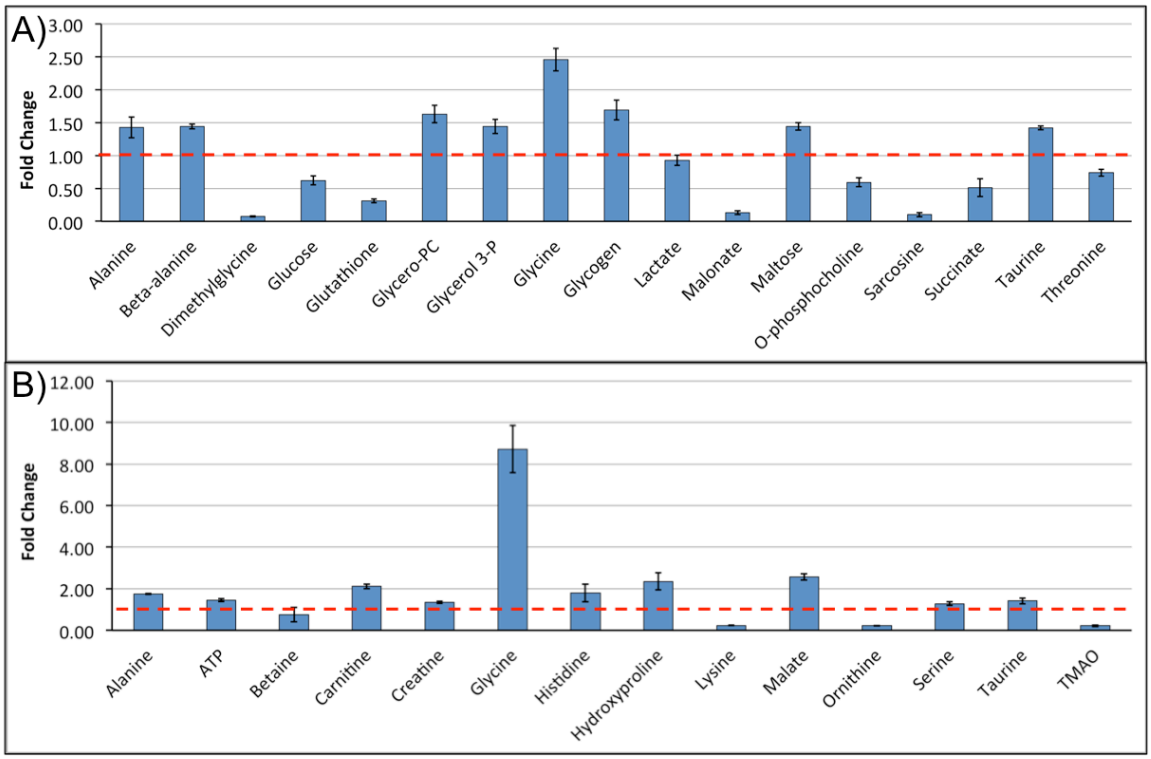
A)
Fold Change
3.00
2.50
2.00
1.50
1.00
0.50
0.00
Alanine
Beta-alanine
Dimethylglycine
Glucose
Glutathione
Glycero-PC
Glycerol 3-P
Glycine
Glycogen
Lactate
Malonate
Maltose
O-phosphocholine
Sarcosine
Succinate
Taurine
Threonine
B)
Fold Change
12.00
10.00
8.00
6.00
4.00
2.00
0.00
Alanine
ATP
Betaine
Carnitine
Creatine
Glycine
Histidine
Hydroxyproline
Lysine
Malate
Ornithine
Serine
Taurine
TMAO

Figure 5.

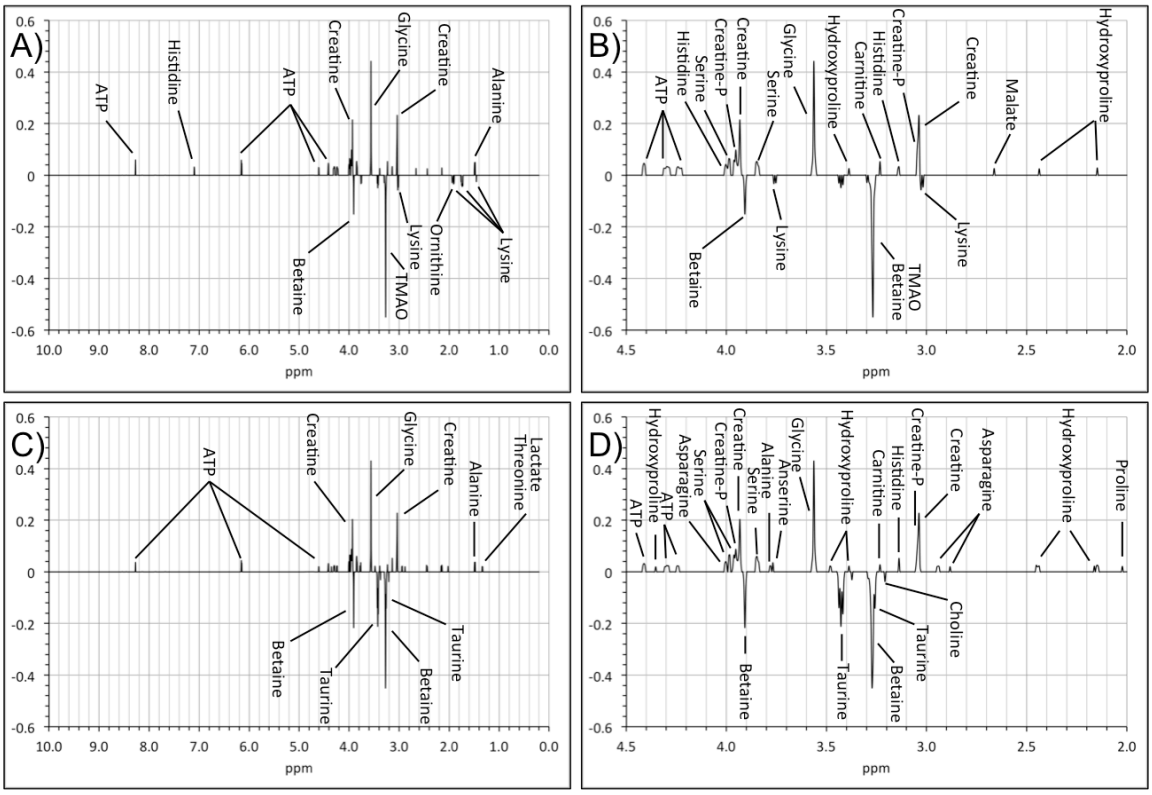
A)
ATP
Histidine
ATP
Creatine
Glycine
Creatine
Alanine
Betaine
Lysine
TMAO
Ornithine
Lysine
ppm
B)
ATP
Histidine
Serine
Creatine-P
Creatine
Glycine
Serine
Hydroxyproline
Histidine
Carnitine
Creatine-P
Creatine
Malate
Hydroxyproline
Betaine
Lysine
TMAO
Betaine
Lysine
ppm
C)
ATP
Creatine
Glycine
Creatine
Alanine
Lactate
Threonine
Betaine
Taurine
Taurine
Betaine
ppm
D)
ATP
Hydroxyproline
ATP
Asparagine
Serine
Creatine-P
Creatine
Serine
Alanine
Anserine
Glycine
Hydroxyproline
Carnitine
Histidine
Creatine-P
Creatine
Asparagine
Hydroxyproline
Proline
Betaine
Taurine
Betaine
Taurine
Choline
ppm

Figure 6.

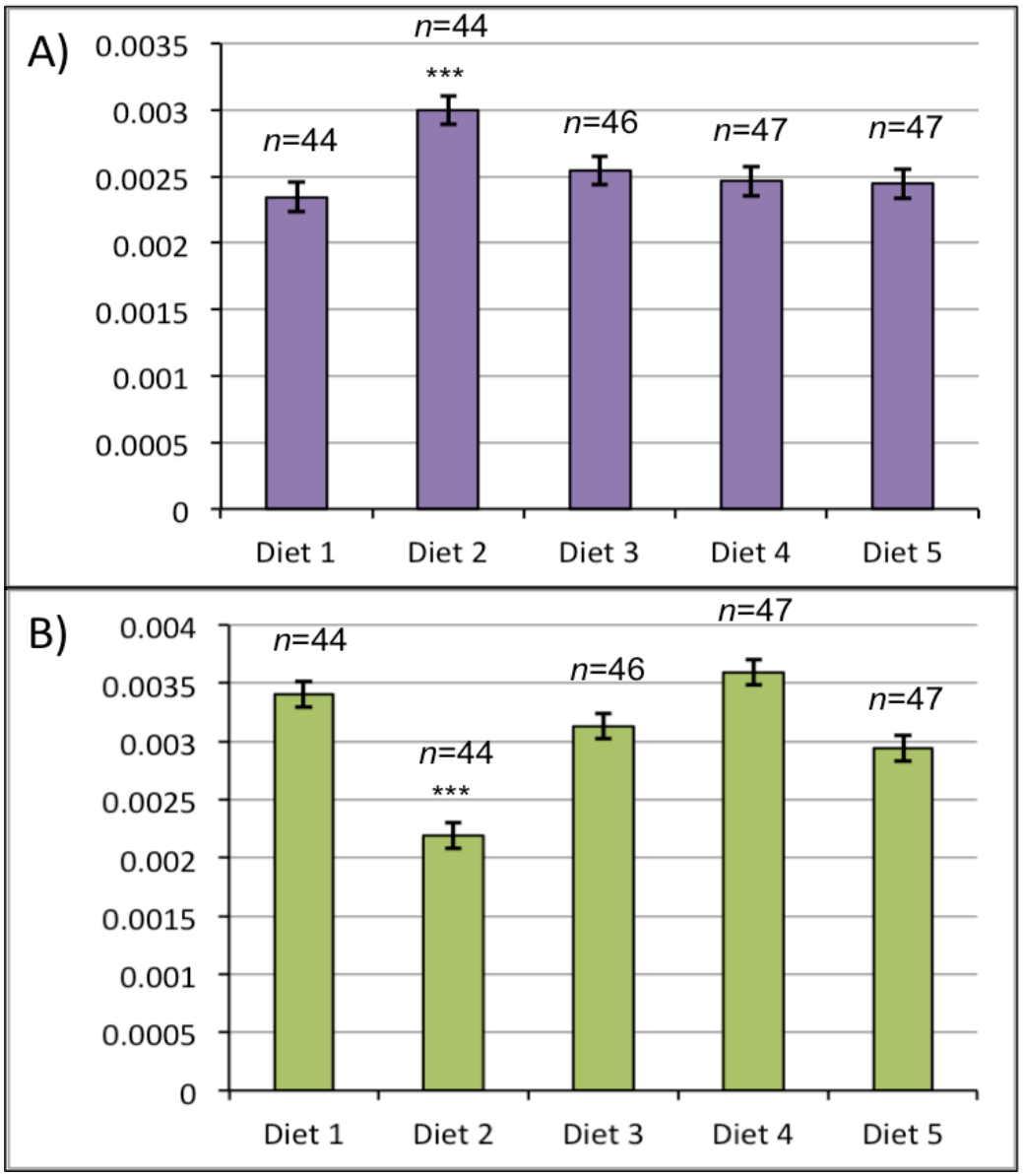
A)
0.0035
0.003
0.0025
0.002
0.0015
0.001
0.0005
0
n=44
***
n=44
n=46
n=47
n=47
Diet 1
Diet 2
Diet 3
Diet 4
Diet 5
B)
0.004
0.0035
0.003
0.0025
0.002
0.0015
0.001
0.0005
0
n=44
n=44
***
n=46
n=47
n=47
Diet 1
Diet 2
Diet 3
Diet 4
Diet 5

Figure 7.

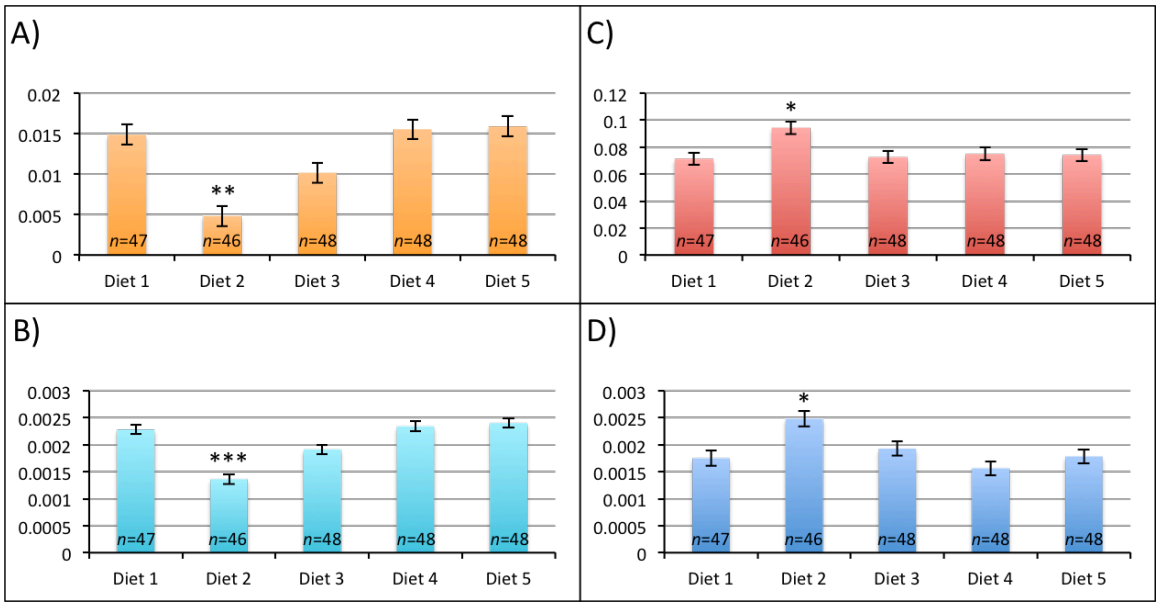
A)
0.02
0.015
0.01
0.005
0
**
n=47
n=46
n=48
n=48
n=48
Diet 1
Diet 2
Diet 3
Diet 4
Diet 5
C)
0.12
0.1
0.08
0.06
0.04
0.02
0
*
n=47
n=46
n=48
n=48
n=48
Diet 1
Diet 2
Diet 3
Diet 4
Diet 5
B)
0.003
0.0025
0.002
0.0015
0.001
0.0005
0
***
n=47
n=46
n=48
n=48
n=48
Diet 1
Diet 2
Diet 3
Diet 4
Diet 5
D)
0.003
0.0025
0.002
0.0015
0.001
0.0005
0
*
n=47
n=46
n=48
n=48
n=48
Diet 1
Diet 2
Diet 3
Diet 4
Diet 5

Figure 8.

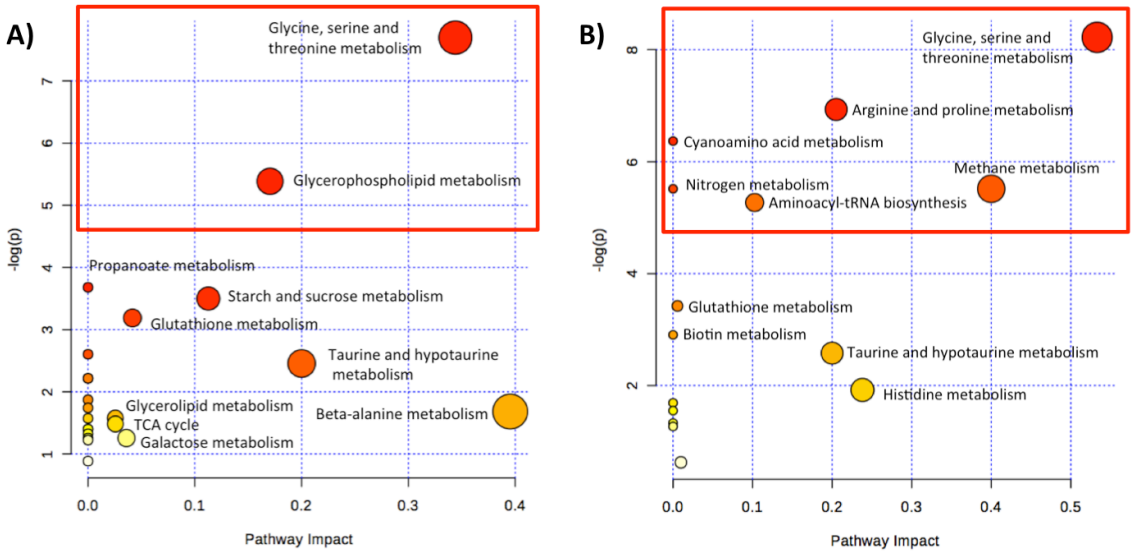
A)
Glycine, serine and threonine metabolism
Glycerophospholipid metabolism
Propanoate metabolism
Starch and sucrose metabolism
Glutathione metabolism
Taurine and hypotaurine metabolism
Glycerolipid metabolism
TCA cycle
Galactose metabolism
Beta-alanine metabolism
-log(p)
Pathway Impact
B)
Glycine, serine and threonine metabolism
Arginine and proline metabolism
Cyanoamino acid metabolism
Methane metabolism
Nitrogen metabolism
Aminoacyl-tRNA biosynthesis
Glutathione metabolism
Biotin metabolism
Taurine and hypotaurine metabolism
Histidine metabolism
-log(p)
Pathway Impact

Figure 9.

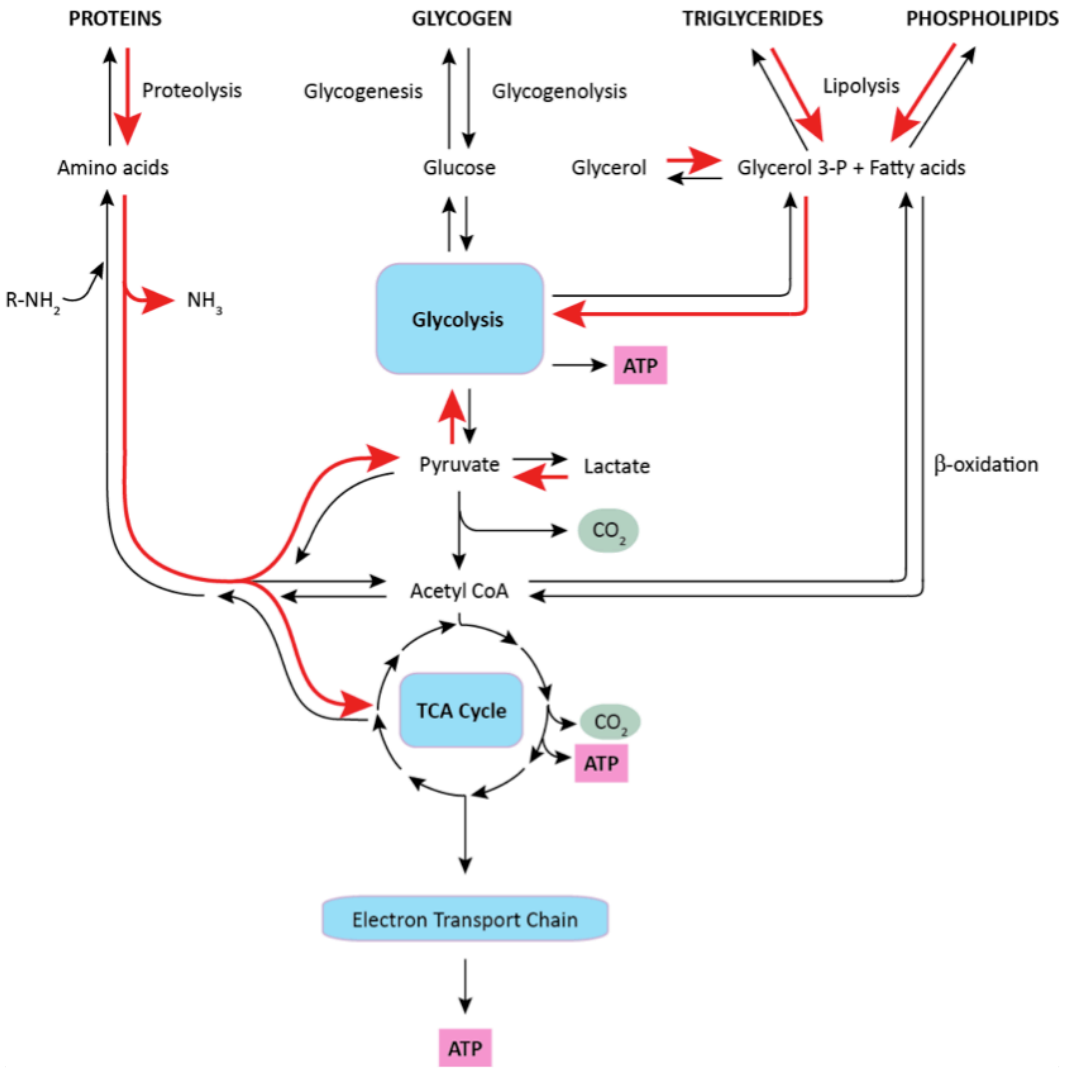
PROTEINS
GLYCOGEN
TRIGLYCERIDES
PHOSPHOLIPIDS
Proteolysis
Glycogenesis
Glycogenolysis
Lipolysis
Amino acids
Glucose
Glycerol
Glycerol 3-P + Fatty acids
R-NH2
NH3
Glycolysis
ATP
Pyruvate
Lactate
β-oxidation
CO2
Acetyl CoA
TCA Cycle
CO2
ATP
Electron Transport Chain
ATP

For Table of Contents Only.